

Experimental demonstration of quantum walk with the walker initially in a superposition state

Qi-Ping Su¹, Yu Zhang¹, Li Yu¹, Jia-Qi Zhou¹, Jin-Shuang Jin¹, Xiao-Qiang Xu¹, Shao-Jie Xiong^{1,3}, Qing-Jun Xu¹, Zhe Sun¹, Kefei Chen², Franco Nori^{4,5*} and Chui-Ping Yang^{1*}

¹*Department of Physics, Hangzhou Normal University, Hangzhou, Zhejiang 310036, China*

²*Department of Mathematics, Hangzhou Normal University, Hangzhou 310036, China*

³*State Key Laboratory of Precision Spectroscopy, Department of Physics,*

East China Normal University, Shanghai 200062, China

⁴*Theoretical Quantum Physics Laboratory, RIKEN Cluster for Pioneering Research, Wako-shi, Saitama 351-0198, Japan and*

⁵*Department of Physics, University of Michigan, Ann Arbor, Michigan 48109-1040, USA*

(Dated: June 12, 2019)

The preparation of the initial superposition state of discrete-time quantum walk (DTQW) is necessary for the research and applications of DTQW. In linear optics, it is always easy to prepare an initial superposition state of the coin, which is encoded by polarization state; while the preparation of a superposition state of the walker is challenging. We here report the first DTQW protocol with the walker's position encoded in polarization space of single photons and the first experimental demonstration of DTQW over six steps with the walker initially in a superposition state, by using only passive linear-optical elements. The effect of the walker's different initial superposition state on the spread speed of the DTQW and on the entanglement between the coin and the walker is also investigated for the first time. It is shown that the properties of DTQW with the walker initially in a superposition states of the walker are very different from those of DTQW starting from a single position. Our findings reveals more properties of DTQW and paves a new avenue to study DTQW.

INTRODUCTION

Quantum walks (QWs) are extensions of the classical random walk [1] and have wide applications in quantum algorithms [2–4], quantum simulation [5–8], quantum computation [9–11], and so on [12, 13]. In standard one-dimensional (1D) discrete-time quantum walks (DTQWs) [14, 15], the walker's position can be denoted as $|x\rangle$ (x is a integer number) and the coin can be described with the basis states $|0\rangle_c$ and $|1\rangle_c$. The evolutions of the walker and the coin are usually characterized by a time-independent unitary operator $U = TS_c(\psi)$. In each step, the coin is tossed by

$$S_c(\psi) = \begin{pmatrix} \cos \psi & -\sin \psi \\ \sin \psi & \cos \psi \end{pmatrix}$$

with $\psi \in (0^\circ, 90^\circ)$, and the walker is shifted by $T = \sum_x |x+1\rangle\langle x| \otimes |1\rangle_c\langle 1| + \sum_x |x-1\rangle\langle x| \otimes |0\rangle_c\langle 0|$. In general, the result of the DTQWs with a finite number of steps is determined by the initial states of the coin and the walker as well as the operator U . The deep investigation of DTQW properties and the effect of the initial states on DTQW is important and necessary for applications of DTQW.

It is worth noting that DTQW with the walker initially in a superposition state has not been demonstrated in experiment. DTQWs have been experimentally realized in several systems, such as linear optics [4–6, 16–18], ion traps [20, 21], cavity quantum electro-dynamics [22],

and neutral atom traps [23]. In these DTQW experiments, the walker always starts from the original position $|0\rangle$. The practicable preparation of initial superposition states of the walker in the most DTQW experiments is a tough job. But initial superposition states of the walker are usually required for applications of DTQW. For example, an initial uniform superposition state of the walker's position is required in the Grover walk [2]. The DTQW with initial superposition states of the walker are quite different from the standard DTQW (i.e., the walker starts from a single position $|x\rangle$), because the final state of the former is coherent superposition of the final states of the standard DTQW starting from different single positions and thus contains more quantum interference.

Especially, we note that the effect of the coin's initial state on DTQW has been well studied [14–19] but the effect of the walker's initial superposition states on DTQW has never been investigated in linear optics. In present linear-optical DTQW implementation schemes [24–26], the coin was always encoded in the polarization state and the position of the walker must be encoded in high dimensional spaces. In [24], the coin was encoded using the polarization state and the walker's positions were encoded using the paths of the photons, in which an additional calcite beam displacer was needed in each step to perform the conditional shift of the walker and DTQWs with up to 6 steps were measured in experiment. In [25], the coin was also encoded using the polarization state and the walker's positions were encoded using the temporal information of single photons, in which the coin operator was adjustable and 5-step DTQWs were studied experimentally. In these works, the preparation of arbitrary initial states of the coin is not hard since it is easy to get arbitrary polarization states using half-wave plates

*Electronic address: yangcp@hznu.edu.cn; fnori@riken.jp

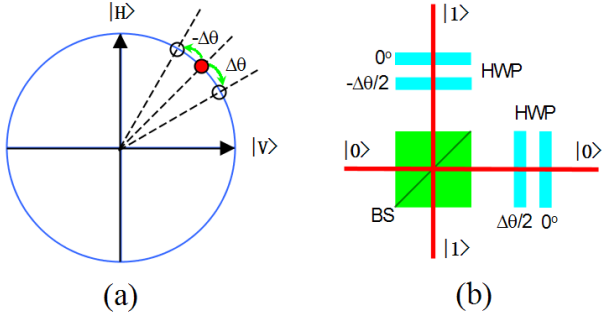


FIG. 1: (color online) (a) The encoding of walker's position and the implementation of conditional translation T_p in the polarization space. $|H\rangle$ ($|V\rangle$) is the horizontal (vertical) polarization state. (b) Optical realization of the time-independent evolution operator $U = T_p S_c$ for DTQW, in which the coin is tossed by the beam splitter (BS) and the conditional transition of walker's positions $|k\rangle_p$ is implemented by two half-wave plates (HWPs) oriented at $\Delta\theta/2$ (for the coin state $|0\rangle$) and $-\Delta\theta/2$ (for the coin state $|1\rangle$) and two 0° HWPs.

(HWPs) and quarter-wave plates (QWPs), but preparation of arbitrary initial superposition states of the walker is difficult. To our knowledge, how to encode the walker's position using the polarization state and how to prepare initial superposition states of the walker by using linear-optical devices have not been reported in both theory and experiment. If the walker's position is encoded using the polarization state, an initial superposition state of the walker can be easily prepared in linear-optical experiment. This is one of the core results obtained in this paper.

In this paper, we report the first DTQW protocol with the walker's position encoded in polarization space of single photons and the first experimental implementation of DTQW with the walker initially in a superposition state. A novel encoding method, together with the design of the linear optical setup, allows us to arbitrarily set the input state of the walker and coin in principle. Final states as well as the probability distribution of an one-dimensional DTQW over 6 steps are obtained in experiment, in which the walker is initially in a superposition state. In this case, the effect of the different walker's initial position states on the spread speed of the walker and on the entanglement between the coin and the walker (i.e., the entropy of the reduced density matrix of the coin) are also studied in experiment for the first time.

RESULTS

Protocol for DTQW with the walker walking in the polarization space. To implement DTQW in polarization space, we make the specific choice of encoding the walker's positions using non-orthogonal states $|k\rangle_p = \cos\theta_k|H\rangle + e^{i\phi_k}\sin\theta_k|V\rangle$ (with integer numbers k) in the polarization space of single photons by setting

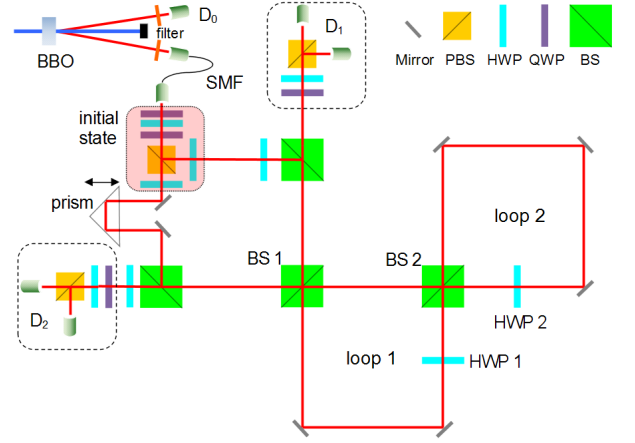


FIG. 2: (color online) Schematic of the experimental setup for quantum walk in the polarization space, in which D_0 is a single-photon detector and D_1 (D_2) represents the standard polarization analysis detector. A pair of photons are generated in the BBO crystal. One photon is detected directly by D_0 as the trigger and another photon is adopted to make DTQW. The initial states of the coin and the walker are prepared in the pink block. The DTQW is realized with two optical loops. The photons experience different steps of DTQW and can be distinguished by their arrival times at D_1 or D_2 after a trigger event.

$\theta_k = k\Delta\theta$ and $\phi_k = 0$. For the details, please see the Method section. The coin is encoded by two paths $|0\rangle$ and $|1\rangle$ of the single photons. As shown in Fig. 1(a), the operator for the conditional translation of $|k\rangle_p$ should be expressed as

$$T_p = \sum_k |k+1\rangle_p \langle k| \otimes |1\rangle \langle 1| + \sum_k |k-1\rangle_p \langle k| \otimes |0\rangle \langle 0|.$$

In this case, the coin operator S_c can be implemented by a $\cos^2\psi/\sin^2\psi$ beam splitter (BS) and the operator T_p can be implemented via two HWPs oriented at 0° and two HWPs oriented at $\Delta\theta/2$ (step forward) and $-\Delta\theta/2$ (step back), as shown in Fig. 1(b). Note that each HWPs oriented at 0° can be replaced by a mirror.

In each step of DTQW in the polarization space, the state of the system is of the form $|\Psi_0\rangle_p|0\rangle + |\Psi_1\rangle_p|1\rangle$, with

$$\begin{aligned} |\Psi_0\rangle_p &= \frac{1}{N_p} \sum_{k=-n}^n a_k |k\rangle_p = \frac{1}{N_a} \sum_{k=-n}^n a'_k |k\rangle_p, \\ |\Psi_1\rangle_p &= \frac{1}{N_p} \sum_{k=-n}^n b_k |k\rangle_p = \frac{1}{N_b} \sum_{k=-n}^n b'_k |k\rangle_p, \end{aligned} \quad (1)$$

where $a'_k = a_k/C_a$, $b'_k = b_k/C_b$, $C_a = \sqrt{\sum |a_k|^2}$, $C_b = \sqrt{\sum |b_k|^2}$, $N_a = N_p/C_a$, $N_b = N_p/C_b$, and N_p is the normalization coefficient which guarantees $\sum_k |a_k|^2 + \sum_k |b_k|^2 = 1$. If one gets all values of a_k and b_k , the probability distribution of the DTQW can be obtained as $|a_k|^2 + |b_k|^2$.

The values of a_k (b_k) can be obtained by using $a_k = C_a a'_k$ ($b_k = C_b b'_k$). Note that $|\Psi_0\rangle_p$ ($|\Psi_1\rangle_p$) has the same

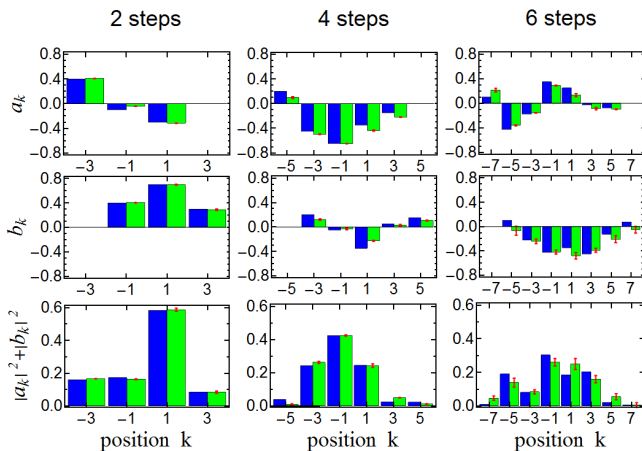


FIG. 3: (color online) Theoretical and experimental results of the 1D Hadamard DTQW after 2, 4, and 6 steps with an initial state of $(0.8|-1\rangle_p + 0.6|1\rangle_p)|0\rangle$. The green (blue) bars represent the experimental (theoretical) results. The red error bars represent statistical errors only.

form as that of $|\Psi\rangle_q$ in the following Eq. (4) and the condition $\sum_k |a'_k|^2 = 1$ ($\sum_k |b'_k|^2 = 1$) is satisfied. By using the encoding method introduced in METHOD section, a'_k and b'_k can be obtained by implementing the DTQW with different angle $\Delta\theta$ one at a time and measuring $|\Psi_0\rangle_p$ and $|\Psi_1\rangle_p$ in path $|0\rangle$ and path $|1\rangle$, respectively. Next, C_a and C_b can be obtained by solving two equations

$$C_a^2 + C_b^2 = 1 \quad \text{and} \quad \frac{C_a^2}{C_b^2} \cdot \frac{|\sum_k a'_k \cos(k\theta)|^2}{|\sum_k b'_k \sin(k\theta)|^2} = r, \quad (2)$$

where $r = |\sum_k a_k \cos(k\theta)|^2 / |\sum_k b_k \sin(k\theta)|^2$ is the ratio between the number of photons counted in path $|0\rangle$ and that counted in path $|1\rangle$ at the same time period for an arbitrary $\theta \neq 0$. With this protocol, DTQW with the walker initially in an arbitrary superposition state or non-superposition state can be easily implemented.

Experimental demonstration of DTQW with the walker initially in a superposition state. A feasible linear-optical setup for DTQW in the photon polarization space is shown in Fig. 2. A pair of photons are generated by the type-I spontaneous parametric down conversion in a 3-mm-thick nonlinear beta-barium borate (BBO) crystal pumped by a 100 mW diode laser (centered at 405.8 nm). One photon is directly detected by detector D_0 as the trigger and the other photon is adopted to make DTQW.

In Fig. 3, we give the results of the 1D Hadamard (i.e., setting $\psi = \pi/4$) DTQW with an initial state of $(0.8|-1\rangle_p + 0.6|1\rangle_p)|0\rangle$. Besides the probability distribution of the walker's position $|a_k|^2 + |b_k|^2$, the coefficients a_k and b_k of the states $|\Psi_0\rangle_p$ and $|\Psi_1\rangle_p$ for a 2-step DTQW, a 4-step DTQW, and a 6-step DTQW are obtained and compared with the theoretical results. Note that the error bars only indicate statistical uncertainty, which are obtained by numerical simulations. The results indicate that the protocol introduced here is realizable in

experiment and DTQW with small errors can be implemented by using the setup shown in Fig. 2.

Since the walker is initially in a superposition state of positions $|-1\rangle_p$ and $|1\rangle_p$, the outermost positions of the walker after an n -step DTQW are denoted by $|-n-1\rangle_p$ and $|n+1\rangle_p$. To simplify the calculation of a_k and b_k , we have used the facts $a_{n+1} = 0$ and $b_{-n-1} = 0$ for this type of DTQW. In this case, only n different $\Delta\theta$ are needed to get a_k and b_k for an n -step DTQW.

The initial state of the walker's position can be easily prepared by rotating angles of the HWPs in our experiment. We have also experimentally study the DTQW with the initial state of $(0.6|-2\rangle_p + |0\rangle_p + 0.8|2\rangle_p)|0\rangle/\sqrt{2}$. The results of reconstructed a_k , b_k and $|a_k|^2 + |b_k|^2$ after 6-step DTQW are shown in Fig. 4, which also fit well with the theoretical results.

Experimental study for the effect of the different initial superposition states of the walker. By means of this DTQW experiment, we also study the relation between the spread speed s and the initial state of the walker's position. The spread speed s is defined as $s(n) = [\sigma(n) - \sigma(0)]/n$, where $\sigma(n)$ is the variance of the position for an n -step DTQW. The results for a 4-step DTQW are obtained and plotted in Fig. 5, in which the initial state is set as $(\alpha|-1\rangle_p + \sqrt{1-\alpha^2}|1\rangle_p)(|0\rangle + i|1\rangle)/\sqrt{2}$ with $\alpha \in (-1, 1)$. It is shown that different initial states of the walker's position will lead to different spread speed of DTQW. Especially, for the DTQWs with α and $-\alpha$ ($\alpha \neq 0$), they have different $\sigma(n)$ and $s(n)$ ($n > 0$) though starting with the same $\sigma(0)$, which is quite different from the classical random walk as shown in Fig. 5, because of the quantum interference.

We also give the simulated relation of $s \sim \alpha$ for 16-step and 50-step DTQW in Fig. 5. It is shown that the properties of the DTQW starting from superposition states of walker are very different from that starting from a single position of walker. For example, the parameter s for $\alpha \neq 0$ approaches a constant more slowly than that for $\alpha = 0$ as the number of DTQW steps increases.

A significant advantage of our DTQW protocol is that the whole final state (and the density matrix) of the coin and the walker's position can be obtained, rather than the position distributions only in other DTQW experimental schemes. In this case, we can investigate the entanglement between the coin and the walker in experiment by calculating the entropy of the reduced density matrix of the coin. The entropy is defined as $E = -\text{Tr}(\rho_c \ln \rho_c)$, where $\rho_c = \text{Tr}_x(\rho_{cx})$ is get by tracing out the walker's position. In Fig. 6, a relation between the entropy E and the walker's initial state from the experiment is compared with the theoretical results for 4-step DTQW. The initial states used here are the same as that for the Fig. 5, whose entropies are 0. It is shown that different initial states of the walker will lead to different entropies after DTQW steps. The results for 16-step and 50-step DTQW are also plotted in Fig. 6. As the number of DTQW steps increases, the entropy will approach a constant value rapidly for all α , not only for

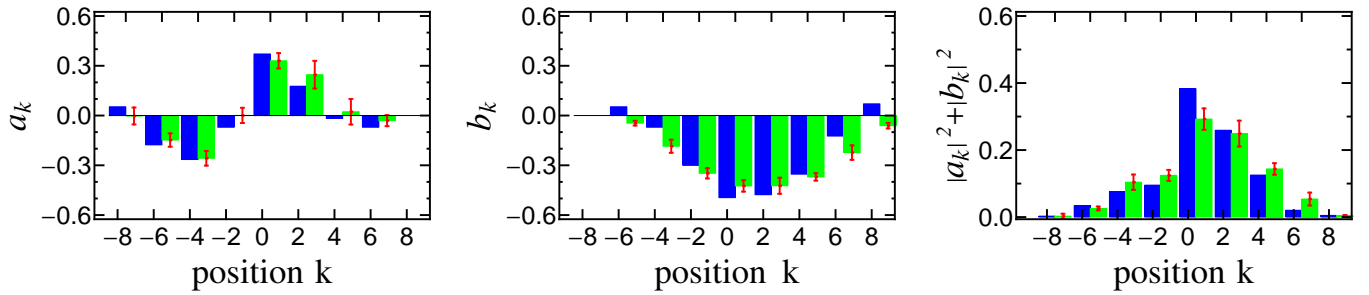


FIG. 4: (color online) Theoretical and experimental results for the 6-step DTQW with an initial state of $(0.6| - 2 \rangle_p + |0 \rangle_p + 0.8|2 \rangle_p)|0 \rangle / \sqrt{2}$. The green (blue) bars represent the experimental (theoretical) results. The red error bars represent statistical errors only.

$\alpha = 0$ [27]. Comparing Fig. 5 with Fig. 6, it implies that a larger spread speed of DTQW corresponds to a larger entanglement between the coin and the walker in general.

DISCUSSION

To implement the DTQW for larger steps, the errors of the experiment should be analyzed and improved. The errors are related to the following factors:

(i) The number of coincidence counts. Because of the leakage of photons at BS 1, the number of coincidence counts will decrease rapidly with increasing of DTQW steps. The ratio of reflection to transmission of all beam splitters adopted in our experiment is 50 : 50. The loss of detected photons after every two steps of DTQW is about 70%. It is an advantage of two optical loops adopted in the setup: photons are leaked and detected after every two steps rather than after each step.

The errors in the experiment can be improved by in-

creasing the number of coincident counts. One method is to replace the 50 : 50 coupler (i.e., BS 1) by a coupler with better ratios. The other method is to increase the number of input photons. This can be achieved in several ways. For example, the BBO can be replaced by a high-efficiency periodically poled KTiOPO4 (PP-KTP), the power of the laser can be improved, or weak laser pulses can be used directly as the input photons of DTQW.

(ii) The quality of the interference in the optical loops. Quantum walks are different from the classical random walks because of the quantum interference. There are two optical loops in the setup. To guarantee good interference of DTQW, optical paths of anticlockwise and clockwise must be adjusted to be the same in each loop and two loops must be adjusted to match with each other. In general, the quality of the interference will become worse with walk steps increasing. An important factor leading to interference degradation is the imperfections of devices, such as the reflections dependence of polarization and nonplanar optical surfaces [24, 25].

To show the scalability of this DTQW protocol and the

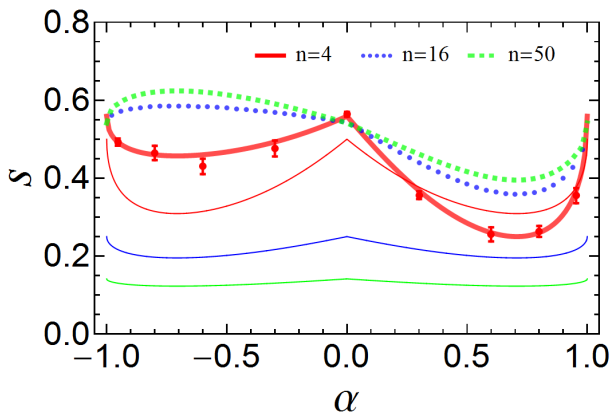


FIG. 5: (color online) The relation between the spread speed s and the initial state of walker's position for 4-step (red), 16-step (blue) and 50-step (green) DTQW. The initial state of DTQW is assumed as $(\alpha| - 1 \rangle_p + \sqrt{1 - \alpha^2}|1 \rangle_p)(|0 \rangle + i|1 \rangle) / \sqrt{2}$. The curves are from theoretical calculation. The thin solid lines are from the corresponding classical random walk for 4, 16, and 50 steps, which have a symmetry on the two sides of $\alpha = 0$. The red dots denote the experimental data and the red error bars represent statistical errors only.

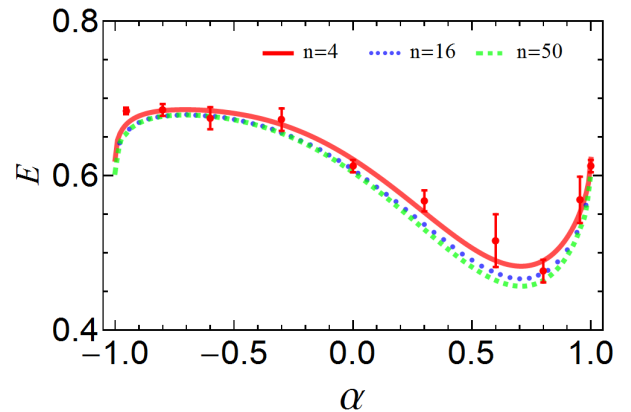


FIG. 6: (color online) The relation between the entropy E and the initial state of the walker's position for 4-step (red), 16-step (blue) and 50-step (green) DTQW. The initial state of DTQW is assumed as $(\alpha| - 1 \rangle_p + \sqrt{1 - \alpha^2}|1 \rangle_p)(|0 \rangle + i|1 \rangle) / \sqrt{2}$. The curves are from theoretical calculation. The red dots denote the experimental data and the red error bars represent statistical errors only.

setup, in the following we estimate the maximum number of steps that are in principle achievable. We assume the use of the perfect devices (including the detectors) and that the loss of detected photons after every two steps of DTQW is 70%. By replacing the 50 : 50 coupler as a 99 : 1 coupler and replacing the input single photons as laser pulses with 1.4W power (5 MHz), there should be ~ 10000 photons detected in one second after 150 steps, provided that the signal-to-noise ratio can be improved by adding an active switch to couple the photon out of the loops.

We have experimentally demonstrated an one-dimensional DTQW with the walker walking in the polarization space of single photons. This work differs from previous works in that the walker is initially in a superposition state and the walker's position is encoded using the polarization state. The ability to operate with different initial superposition states of the walker and to implement DTQWs in a low-dimensional space opens a new avenue for not only discovery of more properties of DTQWs but also extension of DTQW applications.

The encoding method enables one to encode an arbitrary high-dimensional quantum state using a single physical qubit and may be adopted to implement other quantum information tasks. The proposed DTQW protocol is quite general and can be applied to other quantum systems (e.g., cavity or circuit QED systems). Moreover, this work may be extended to realize multi-dimensional DTQWs, which is of importance in the large-scale quantum computing based on quantum walks.

METHOD

The encoding method. Suppose there is an n -dimensional state

$$|\Psi\rangle = \sum_{k=1}^n a_k |k\rangle \quad \text{with} \quad \sum_{k=1}^n |a_k|^2 = 1, \quad (3)$$

in which $|k\rangle$ ($k = 1, 2, \dots, n$) are orthogonal states. In the following, we will propose a method to encode this state with a two-dimensional qubit and to read out all a_k from the qubit by measurement. The obtained a_k can be used to reconstruct the n -dimensional state $|\Psi\rangle$ of Eq. (3).

The state $|\Psi\rangle$ can be encoded by using n non-orthogonal states $|k\rangle_q = \cos\theta_k|0\rangle + e^{i\phi_k}\sin\theta_k|1\rangle$ ($k = 1, 2, \dots, n$) of a qubit, which correspond to n different points in the Bloch sphere of the qubit. With $|k\rangle$ replaced by $|k\rangle_q$, the state of the qubit in the encoded state can be expressed as

$$|\Psi\rangle_q = \frac{1}{N_q} \sum_{k=1}^n a_k |k\rangle_q = \frac{1}{N_q} (C_0|0\rangle + C_1|1\rangle), \quad (4)$$

where $C_0 = \sum_{k=1}^n a_k \cos\theta_k$, $C_1 = \sum_{k=1}^n a_k e^{i\phi_k} \sin\theta_k$, and $N_q = \sqrt{|C_0|^2 + |C_1|^2}$. Note that the same state $|\Psi\rangle_q$ can be constructed by performing suitable operations on an initial state of the qubit, which is just the case considered in the above DTQW protocol.

We now show how to read out a_k from $|\Psi\rangle_q$. The density matrix of the encoded state $|\Psi\rangle_q$ can be expressed as

$$\rho_q = \frac{1}{N_q^2} \begin{pmatrix} C_0^* C_0 & C_1^* C_0 \\ C_0^* C_1 & C_1^* C_1 \end{pmatrix}, \quad (5)$$

which can be easily obtained by using tomographic measurement on the qubit. Then one homogeneous equation of a_k can be obtained

as

$$C_0 - R \cdot C_1 = 0 \Rightarrow \sum_{k=1}^n (\cos\theta_k - R \cdot e^{i\phi_k} \sin\theta_k) \cdot a_k = 0, \quad (6)$$

where $R = C_0/C_1$ is obtained from the measured ρ_q as

$$R = \rho_{q11}/\rho_{q21} = \rho_{q12}/\rho_{q22}. \quad (7)$$

In this way, $n - 1$ homogeneous equations for a_k can be obtained by repeatedly encoding the state $|\Psi\rangle$ onto a qubit with $n - 1$ different sets $\{|1\rangle_q^j, |2\rangle_q^j, \dots, |n\rangle_q^j\}$ (where $j = 1, 2, \dots, n - 1$, and $|k\rangle_q^j = \cos\theta_k^j|0\rangle + e^{i\phi_k^j}\sin\theta_k^j|1\rangle$), and by measuring the corresponding R^j one at a time. Then a_k ($k = 1, \dots, n$) can be solved from the $n - 1$ homogeneous equations

$$\sum_{k=1}^n (\cos\theta_k^j - R^j \cdot e^{i\phi_k^j} \sin\theta_k^j) \cdot a_k = 0 \quad (8)$$

and the normalization condition $\sum_{k=1}^n |a_k|^2 = 1$. Now the n -dimensional encoded state can be reconstructed by the obtained a_k . This reconstructing process is similar to the reconstruction of density matrix from the tomographic measurement.

To exhibit the generality and scalability of this encoding method, we calculate the fidelity between a random 50-dimensional encoded state and its reconstructed state from the simulation of the encoding process, in which random errors of measured R^j within $\pm 10\%$ are assumed and a specific choice of the non-orthogonal states

$$|k\rangle_q^j = \cos(jk\Delta\theta)|0\rangle + e^{i\Delta\phi} \sin(jk\Delta\theta)|1\rangle \quad (9)$$

is used (i.e., $\theta_k^j = jk\Delta\theta$ and $\phi_k^j = k\Delta\phi$). The averaged fidelity over 1000 random simulations is obtained and its dependence on $\Delta\theta$ and $\Delta\phi$ is plotted in Fig. 7. In the $\sim 41\%$ area of Fig. 7, the averaged fidelity is larger than 90%. It is not hard to find suitable θ_k and ϕ_k to implement the encoding method, and high fidelity can be obtained for encoding large dimensional states if measurement errors are not very large.

With the form of the non-orthogonal states (9), we experimentally demonstrate the encoding and reading of a 16-dimensional state in linear optics system. At first, we encode a uniform state $\Phi_{16} = \frac{1}{4} \sum_{k=1}^{16} |k\rangle$ in the 2-dimensional polarization space of single photons by using $\Delta\theta = 22^\circ$ and $\Delta\phi = 12^\circ$. This encoding can be easily implemented by injecting photons into an adjusted setup consisting of two QWPs and one HWP, which can be used to construct an arbitrary one-qubit gate. Then density matrixes of the encoding photons can be measured and the initial uniform

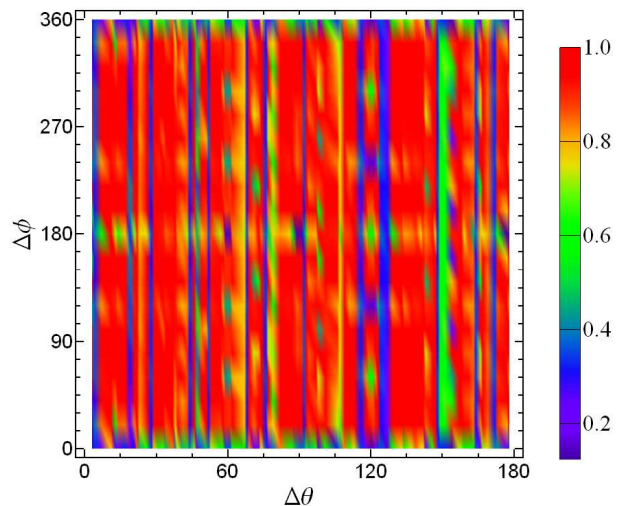


FIG. 7: (color online) Numerical simulations for the fidelity of the encoding of 50 dimensional states into qubits.

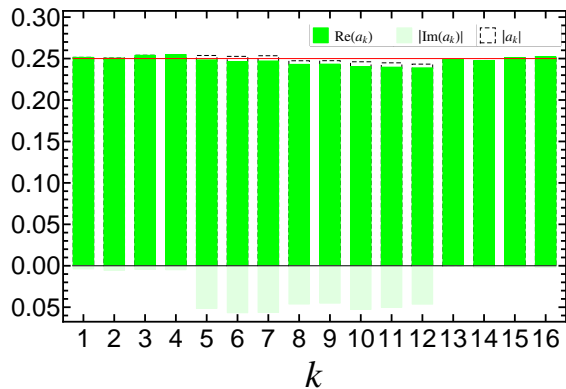


FIG. 8: (color online) Experimental results for the reconstruction of a 16 dimensional state $\frac{1}{4} \sum_{k=1}^{16} |k\rangle$ from encoded single photons in a linear-optical system.

state can be reconstructed. The experimental results of the reconstructed state is shown in Fig. 8, and a high fidelity of 99.1% is achieved. The encoding method introduced in this paper is feasible for the present technology of linear optics and can be easily applied in other quantum systems. The key advantage for the use of this encoding method is the simplicity of setup, because only one physical qubit is required.

The implementation of DTQW in the setup. As shown in Fig. 2, steps of the DTQW are as follows:

(i) Preparation of the initial states of the coin and the walker. An arbitrary coin state can be initialized by a combination of a polarizing beam splitter (PBS), a quarter-wave plate (QWP), and a HWP. An arbitrary state of the walker's position is represented as a polarization state, which can be easily initialized by using two HWPs on the two paths of the DTQW photon after the PBS. Note that lengths of the two paths from the PBS to BS 2 should be the same by adjusting the prism. A proportional-integral-derivative (PID) system can be adopted to stabilize this equivalence of path lengths by using a piezoelectric transducer.

(ii) Steps for implementing the DTQW. The DTQW starts as the photon enters BS 2 for the first time and is implemented in loop 1 and loop 2. In each loop, the anticlockwise and clockwise photon paths are adjusted to overlap with each other and the loop length

is designed to be ~ 30 cm. Here the loop's interference visibility is measured as $\sim 98.5\%$. The steps for the DTQW realization are described below:

Step 1: As the photon passes through BS 2, the coin state is tossed by the operator S_c . The photon after BS 2 will rotate anticlockwise (or clockwise) in the loop 2, and the walker achieves a rotation of $\Delta\theta$ (or $-\Delta\theta$) in the polarization space via HWP 2, just like that shown in Fig. 1(a).

Step 2: Then the photon goes through BS 2 at the second time and the coin is tossed once again. After BS 2, one possibility is that the photon will rotate anticlockwise (or clockwise) in the loop 1 and the walker's state achieves a rotation of $\Delta\theta$ (or $-\Delta\theta$) in the polarization space via HWP 1. The photon will enter BS 2 one more time, and the next step of DTQW will start. The other possibility is that the photon goes through BS 1 and then is detected by D_1 (D_2) to get a_k (b_k) for a 2-step DTQW.

(iii) Extracting the final state of a 2n-step DTQW. The final state of a 2n-step DTQW can be obtained by measuring the photons which are detected after repeating steps 1 and 2 for n times. Because the total length of loop 1 and loop 2 is about 60 cm, the time gap between the photon detection after a $(2n - 2)$ -step DTQW and the photon detection after a 2n-step DTQW is ~ 2 ns. In this case, the time window of the coincidence detections between D_0 and D_1 (D_2) is set as 0.49 ns.

Acknowledgments

This work is supported in part by the NKRDP of China (Grant No. 2016YFA0301802) and the National Natural Science Foundation of China under Grant Nos [11504075, 11374083, 11774076]. This work is partially supported by the MURI Center for Dynamic Magneto-Optics via the AFOSR Award No. FA9550-14-1-0040, the Army Research Office (ARO) under grant number 73315PH, the AOARD grant No. FA2386-18-1-4045, the IMPACT program of JST, CREST Grant No. JPMJCR1676, JSPS-RFBR Grant No. 17-52-50023.

-
- [1] Y. Aharonov, L. Davidovich, and N. Zagury, Quantum random walks, *Phy. Rev. A* 48, 1687 (1993).
 - [2] N. Shenvi, J. Kempe, and K. B. Whaley, Quantum random-walk search algorithm, *Phys. Rev. A* 67, 052307 (2003).
 - [3] C. D. Franco, M. M. Gettrick, and T. Busch, Mimicking the probability distribution of a two-dimensional Grover walk with a single-qubit coin, *Phys. Rev. Lett.* 106, 080502 (2011).
 - [4] Y.-C. Jeong, C. D. Franco, H.-T. Lim, M. S. Kim, and Y.-H. Kim, Experimental realization of a delayed-choice quantum walk, *Nat. Comm.* 4, 2471, (2013).
 - [5] A. Crespi, et al., Anderson localization of entangled photons in an integrated quantum walk, *Nat. Photon.* 7, 322 (2013).
 - [6] X. Zhan, L. Xiao, Z. H. Bian, K. K. Wang, X. Z. Qiu, B. C. Sanders, W. Yi, and P. Xue, Detecting Topological Invariants in Nonunitary Discrete-Time Quantum Walks, *Phys. Rev. Lett.* 119, 130501 (2017).
 - [7] A. Peruzzo, et al., Quantum walks of correlated photons, *Science* 329, 1500 (2010).
 - [8] T. Kitagawa, M. S. Rudner, E. Berg, and E. Demler, Exploring topological phases with quantum walks, *Phys. Rev. A* 82, 033429 (2010).
 - [9] A. M. Childs, Universal computation by quantum walk, *Phys. Rev. Lett.* 102, 180501 (2009).
 - [10] M. S. Underwood and D. L. Feder, Universal quantum computation by discontinuous quantum walk, *Phys. Rev. A* 82, 042304 (2010).
 - [11] A. M. Childs, D. Gosset, and Z. Webb, Universal computation by multiparticle quantum walk, *Science* 339, 791 (2013).
 - [12] P. Kurzynski and A. Wojcik, Quantum walk as a generalized measuring device, *Phys. Rev. Lett.* 110, 200404 (2013).
 - [13] P. Reberntrost, M. Mohseni, I. Kassal, S. Lloyd, and A. A. Guzik, Environment-assisted quantum transport, *New J. Phys.* 11, 033003 (2009).

- [14] J. Kempe, Quantum random walks: an introductory overview, *Conte. Phys.* 44, 307 (2003).
- [15] S. E. Venegas-Andraca, Quantum walks: a comprehensive review, *Quan. Inf. Proc.* 11, 1015 (2012).
- [16] P. Xue, R. Zhang, H. Qin, X. Zhan, Z. H. Bian, J. Li, and B. C. Sanders, Experimental quantum-walk revival with a time-dependent coin, *Phys. Rev. Lett.* 114, 140502 (2015).
- [17] B. Do, M.L. Stohler, S. Balasubramanian, D.S. Elliott, C. Eash, E. Fischbach, M.A. Fischbach, A. Mills, B. Zwickl, Experimental realization of a quantum quincunx by use of linear optical elements, *Opt. Soc. Am. B* 22, 020499 (2005).
- [18] L. Sansoni, et al., Two-particle bosonic-fermionic quantum walk via integrated photonics, *Phys. Rev. Lett.* 108, 010502 (2012).
- [19] P. Xue and B. C. Sanders, Two quantum walkers sharing coins, *Phys. Rev. A* 85, 022307 (2012).
- [20] H. Schmitz, R. Matjeschk, C. Schneider, J. Glueckert, M. Enderlein, T. Huber, and T. Schaetz, Quantum walk of a trapped ion in phase space, *Phys. Rev. Lett.* 103, 090504 (2009).
- [21] F. Zahringer, G. Kirchmair, R. Gerritsma, E. Solano, R. Blatt, and C.F. Roos, Realization of a quantum walk with one and two trapped ions, *Phys. Rev. Lett.* 104, 100503 (2010).
- [22] E. Flurin, V. V. Ramasesh, S. Hacoen-Gourgy, L. S. Martin, N. Y. Yao, and I. Siddiqi, Observing Topological Invariants Using Quantum Walks in Superconducting Circuits, *Phys. Rev. X* 7, 031023 (2017).
- [23] M. Karski, L. Forster, J.-M. Choi, A. Steffen, W. Alt, D. Meschede, and A. Widera, Quantum walk in position space with single optically trapped atoms, *Science* 325, 174 (2009).
- [24] M.A. Broome, A. Fedrizzi, B.P. Lanyon, I. Kassal, A. Aspuru-Guzik, and A.G. White, Discrete single-photon quantum walks with tunable decoherence, *Phys. Rev. Lett.* 104, 153602 (2010).
- [25] A. Schreiber, K. N. Cassemiro, V. Potocek, A. Gabris, P.J. Mosley, E. Andersson, I. Jex, and Ch. Silberhorn, Photons walking the line: a quantum walk with adjustable coin operations, *Phys. Rev. Lett.* 104, 050502 (2010).
- [26] D. Bouwmeester, I. Marzoli, G.P. Karman, W. Schleich, and J.P. Woerdman, Optical galton board, *Phys. Rev. A* 61, 013410 (1999).
- [27] I. Carneiro, M. Loo, X. Xu, M. Girerd, V. Kendon and P. L. Knight, Entanglement in coined quantum walks on regular graphs, *New J. Phys.* 7 (2005) 156.